

A search for a short-lived axion decaying to e^+e^- in a 20 GeV photoproduction experiment*

SLAC Hybrid Facility Photon Collaboration:

E. S. Ackleh,^j J. E. Brau,^{j°} J. M. Butler,^{f‡} K. C. Moffeit,^f P. Rankin,^{f§}
K. Abe,^g R. Armenteros,^{f°} T. C. Bacon,^c J. Ballam,^f H. H. Bingham,ⁱ K. Braune,^{f°}
D. Brick,^b W. M. Bugg,^j W. Cameron,^c H. O. Cohn,^d D. C. Colley,^a G. T. Condo,^j
P. Dingus,ⁱ R. Erickson,^f T. Fieguth,^f R. C. Field,^f B. Franek,^e R. Gearhart,^f
T. Glanzman,^f I. M. Godfrey,^c J. J. Goldberg,^{fΔ} G. Hall,^c E. R. Hancock,^e
T. Handler,^j H. J. Hargis,^j E. L. Hart,^j M. J. Harwin,^c K. Hasegawa,^g M. Jobes,^a
T. Kafka,^h G. E. Kalmus,^e D. P. Kelsey,^e T. Kitagaki,^g W. A. Mann,^h R. Merenyi,^{h‡}
R. Milburn,^h J. J. Murray,^f A. Napier,^h V. O'Dell,^b H. Sagawa,^g J. Schneps,^h
S. J. Sewell,^e J. Shank,ⁱ A. M. Shapiro,^b J. Shimony,^j K. Tamai,^g S. Tanaka,^g
D. A. Waide,^a M. Widgoff,^b S. Wolbers,^{f‡} C. A. Woods,^{c#} A. Yamaguchi,^g
G. P. Yost,ⁱ and H. Yuta^g

- a. Birmingham University, Birmingham, B15 2TT, England
- b. Brown University, Providence, Rhode Island 02912 USA
- c. Imperial College, London, SW7 2BZ, England
- d. Oak Ridge National Laboratory, Oak Ridge, Tennessee 37830 USA
- e. Rutherford Appleton Laboratory, Didcot, Oxon OX11 0QX, England
- f. Stanford Linear Accelerator Center, Stanford University, Stanford, California 94309 USA
- g. Tohoku University, Sendai 980, Japan
- h. Tufts University, Medford, Massachusetts 02155 USA
- i. University of California, Berkeley, California 94720 USA
- j. University of Tennessee, Knoxville, Tennessee 37916 USA

Present address:

- ◇ CERN, Geneva 23, Switzerland
- † American Dade Co., Costa Mesa, California 92660 USA
- ‡ Fermilab, P.O. Box 500, Batavia, Illinois 60510 USA
- ‡ Analytical Sciences Corp., Reading, Massachusetts 01867 USA
- # Langton EPS, London, England
- ° Dept. of Physics, University of Oregon, Eugene, Oregon 97403 USA
- § Dept. of Physics, University of Colorado, Boulder, Colorado 80309 USA
- Δ On leave from Technion-Israel Institute of Technology, Haifa, Israel.

Submitted to *Physical Review D*.

* Work supported in part by the Department of Energy, contract DE-AC03-76SF00515; the Japan-U.S. Cooperative Research Project on High Energy Physics under the Japanese Ministry of Education, Science and Culture; the UK Science and Engineering Research Council; and the U.S. National Science Foundation.

ABSTRACT

We have searched for evidence of the decays of a short-lived particle which mixes with neutral pions and decays to e^+e^- pairs. The search was made in the data from a 20 GeV photoproduction experiment at the SLAC Hybrid Facility, in which e^+e^- pairs originating close to the production vertex (covering axion lifetimes in the range of $10^{-15} \text{ sec} < \tau < 10^{-11} \text{ sec}$) could be directly observed. A signal for such an axion would be an excess of e^+e^- pairs relative to the number of expected photon conversions. Although we consider specifically the axion variant recently proposed by Peccei *et al.*, and by Krauss and Wilczek, which couples strongly to u -quarks only, we are also sensitive to any particle with a sufficiently strong coupling to π^0 's. No measurable excess of e^+e^- pairs is observed and we put limits on the allowed range of the π^0 coupling as a function of the particle's mass and lifetime.

I. INTRODUCTION

The axion was introduced¹ about ten years ago in order to explain why the CP phase arising in the quark mass matrix in QCD was determined experimentally to be close to zero.² The axion is the result of postulating an additional chiral symmetry [known as the Peccei–Quinn (PQ) symmetry] which gives a natural mechanism for generating zero values for the phase. Although this particular axion has been conclusively ruled out by experiment,³ the axion concept is still of considerable interest to theorists. One class of proposed models⁴ increases the scale of the PQ symmetry breaking, thus reducing the axion’s mass (resulting in axions which may be responsible for the dark matter in the universe). Another group of models, mainly inspired by the observation of narrow correlated peaks in the e^+ and e^- spectra from heavy ion collisions at GSI,⁵ predict more massive, shorter-lived axions.

The models proposing the existence of these latter type of axions (due to Peccei *et al.*,⁶ and Krauss and Wilczek⁷), highlighted the existence of a region of mass-lifetime space which had not then been subjected to a direct search for particles. We report here on a study which was motivated by the possible existence of such variant axions. However, since we searched for an excess of e^+e^- pairs compared to the number expected from conventional (known) sources, our limits are not dependent on the assumption that the particle is an axion.

The GSI data suggest the existence of a 1.8 MeV object which decays into e^+e^- pairs with a lifetime of less than 10^{-9} sec. Constraints on axion production set by beam dump experiments are avoided in variant axion models by making their lifetimes so short (typically about 5×10^{-13} sec) that the majority of produced axions would have decayed in the dump. In order to avoid constraints on axion production from

heavy quark decays,⁸ only the axion's coupling to the u -quark and to the electron is made large. The coupling to all other fermions is weak since it is given by the inverse of the u -coupling. Finally, the strong limits resulting from measurements of $g-2$ for muons are replaced by the weaker limits from electron $g-2$ measurements⁹ since these models violate $e-\mu$ universality.

Any process Y (γp interactions, for example), which produces π^0 's will also produce these axions according to the general relation (in the limit where $\xi_\pi^2 \ll 1$):

$$d\sigma(Y \rightarrow aX) = \xi_\pi^2 d\sigma(Y \rightarrow \pi^0 X) \quad ,$$

where ξ_π^2 is a measure of the *axion* - π mixing and is given by¹⁰

$$\xi_\pi^2 = \frac{1}{4m_u m_d} [(3m_d - m_u) \sin^2 \alpha - (3m_u - m_d) \cos^2 \alpha]^2 \frac{m_a^2}{m_\pi^2} \quad ,$$

where m_u and m_d are the u and d quark masses, m_a is the axion mass, m_π is the π^0 mass, and α is some unknown angle. The m_u and m_d dependence is a result of the axions coupling via the Higgs fields responsible for giving the u and d quarks mass.

Current algebraic calculations give m_u and m_d ,¹¹ but the phase α is not predictable. If the coupling to π^0 's were zero, then we would have no sensitivity to axions. This would occur, for example, if the phase angle α took a value of about 0.5 rad (using the calculated values of m_u and m_d).¹²

However, for the class of variant axion models of particular interest here which have a fundamental coupling only to u -quarks, the $a-\pi$ mixing parameter simplifies to

$$\xi_\pi^2 \approx \frac{1}{2} \frac{m_a^2}{m_\pi^2} \quad (1)$$

which gives $\xi_\pi^2 \approx 9 \times 10^{-5}$ for $m_a = 1.8 \text{ MeV}/c^2$.¹³

In this paper, we do not assume any relationship between axion mass and lifetime. We do assume, however, that the dominant decay mode is into e^+e^- pairs. Since the particle is predicted to be short-lived, restricting the search to a region close to the production vertex enhances the chance of observing a signal over the background due to γ conversions. In addition, we use information on the invariant mass of the e^+e^- pairs to improve our sensitivity.

II. EXPERIMENTAL DETAILS AND DATA SELECTIONS

This study is based on a sample of approximately 140K hadronic events. All of the events having a secondary vertex (approximately 13K events, about 5K of which contained charged decays) were reconstructed, including those with close two-prong decays or conversions. The apparatus used for this experiment (BC75) has been described in detail elsewhere.¹⁴ However, one feature is especially relevant to this analysis. The bubble chamber was equipped with two high resolution (HRO) cameras, each capable of 30 μm resolution, in addition to the usual three normal resolution stereo ones. This system photographed bubbles of about 40 μm diameter, which greatly enhanced our ability to resolve tracks coming from secondary vertices close to the primary event vertex. This allowed us to detect the decay of short-lived particles (with typical decay lengths of a few mm) and to see photon conversions to e^+e^- pairs close to the primary vertex. In effect, BC75 functions as the inverse of a beam dump experiment since a study is made of decays in the target, not of the particles some distance away from their production point. It therefore tends to be sensitive to a complementary region of mass-lifetime space.

The scanning procedure went as follows: first, the low-resolution film was twice scanned for hadronic interactions (the scanning efficiency was found to be $99 \pm 1\%$).

The scan region on the HRO film was then studied for evidence of decays within 1.5 cm of the primary vertex. In order for an event to be studied more closely, clear evidence was required either of a neutral decay vertex or of a track which did not point back to the primary vertex. All events passing either of these criteria became candidates and were measured and entered onto a candidate data summary tape (DST). The neutral decays were predominantly two-prong V^0 's, which were identified as K^0 or Λ decays, and γ conversions. The sample of K^0 's and Λ 's was used to investigate the scanning efficiency in this region by comparing the number of decays found to the number predicted using a control region. The scanning efficiency for strange particles was above 95%.¹⁴

The present analysis concentrates on the observed "photon" conversions. A photon was defined as any particle with a two-prong decay where the decay products had a reconstructed mass $m_{e^+e^-} < 30 \text{ MeV}/c^2$. The measurement error on $m_{e^+e^-}$ is normally about $3 \text{ MeV}/c^2$. Events with badly measured tracks were rejected (a loss of less than 3% from the final sample). To ensure high and uniform detection efficiency, the secondary vertex was required to be at least 1 mm from the primary event vertex. Below 1 mm, the detection efficiency is reduced because of confusion between tracks from the primary vertex and e^+e^- pairs pointing to the vertex. The scanning efficiency for the pairs in the accepted sample is shown as a function of the distance from the primary vertex to the pair's origin in Fig. 1, confirming that the efficiency is high and uniform in the 1-15 mm region. The scanning efficiency (for the combined scans) for these events has been calculated using a maximum likelihood method to be $95 \pm 1\%$. This efficiency is consistent with all other estimates made of scanning efficiency in this region.¹⁴

Figure 2 shows the reconstructed mass distribution for e^+e^- pairs in a 40–200 mm scan region for a sample of data from an earlier experiment of this collaboration, BC72/73.¹⁵ BC72/73 used the same beam and nearly the same apparatus¹⁶ as BC75 but was not restricted to a study of events with close secondary vertices. This data provides information on the expected number of conversions and the calculated invariant mass of the e^+e^- pairs in the *absence* of short-lived particles. The data in Fig. 3 shows the reconstructed e^+e^- mass distribution for data from BC75 measured in the same way as the data from BC72/73 shown in Fig. 2 but restricted to pairs found within 1–15 mm of the primary vertex. The solid curves on Figs. 2 and 3 show a four parameter fit to the BC72/73 data used in this analysis and described in the appendix. It is important to note that the BC72/73 and the BC75 distributions are consistent with each other. The apparent discrepancy in the lowest mass bin in Fig. 3 is due to an imperfection in the parameterization. After the length and mass cuts, 277 e^+e^- pairs remain from the BC75 data. The length distribution is shown in Fig. 4. We would like to stress that this distribution agrees with that expected for photon conversions in hydrogen giving a χ^2 of 8.09 for 14 degrees of freedom, and shows no evidence for a short-lived axion component.

The data also has an integrated sum consistent with our expectations. In order to calculate how many photon conversions with a particular invariant mass would be expected in this short decay region in the absence of axion production, we need data from a ‘control decay’ region. As mentioned earlier, this data was provided by experiment BC72/73. Using all the longer lived V^0 's found in the control decay region which satisfied the same mass cuts as our 277 event sample, we could extrapolate back to find the expected distribution for our data sample in the *absence* of a short-lived component. Allowing for the difference in sensitivity to hadronic events 287 ± 20 photon

conversions are expected in the region $1 < l < 15$ mm. More details of the control signal and normalization can be found in the appendix. We conclude that the observed number of photons is completely compatible with the assumption that there is no production of axions within the limits of our sensitivity.

III. LIMITS ON AXION PRODUCTION

Our analysis can be divided into two parts. First, we demonstrate that we could in principle have detected the existence of axions in a particular region of mass-lifetime space. We compare predicted distributions of e^+e^- pair conversion lengths from the decays of π^0 's and an assumed axion with the expected distributions from π^0 decay γ 's alone. We apply a cut on the invariant mass of the e^+e^- pair around the assumed axion mass to increase our sensitivity to higher mass axions. We have performed a Monte Carlo study to assess the significance of this comparison. This Monte Carlo study is described in detail in the appendix. We find, as described below, that evidence for the excess of pairs from the decay of an axion could be distinguished from the conversions of photons from pion decay alone over substantial region of the possible axion lifetime-mass space for given values of ξ_π . (We refer to this region as the *region of potential sensitivity*.)

Second, we compare our actual measured length distributions (after applying a mass cut) with the theoretical expectations as a function of the axion lifetime and mass to determine the excluded values of these parameters. (We refer to this region as the *region of exclusion*.)

The significance of the comparison of the data with the null hypothesis (no axion source) has been determined by generating 2000 Monte Carlo experiments for each of

various values of the axion lifetime and mass and comparing the length distribution of each experiment with a null hypothesis, generated by assuming all e^+e^- pairs come from the conversion of photons produced by π^0 decay. The number of axions, N_a , is chosen according to the prescription given in Eq. 2. The number of γ 's from π^0 decays is based on the data from BC72/73, corrected for the possible presence of axions in that data. The axions decay according to a distribution based on

$$\frac{dN_a}{dl} = m_a/p_a\tau_a N_a^{tot} e^{-lm_a/p_a\tau_a} ,$$

where N_a^{tot} is the total number of axions produced, p_a and τ_a are the axion momentum and lifetime, respectively, and p_a is chosen to agree with the measured momentum distribution of the π^0 's. Those axions within the region of acceptance (1–15 mm) are then added to the gamma sample. For each experiment, the χ^2 of the fit of the Monte Carlo data to the length distribution of the null hypothesis is calculated to determine the distribution of χ^2 values for the lifetime/mass point. The null hypothesis is rejected if the χ^2 exceeds 21.1 (90% confidence level for 14 degrees of freedom). Figure 5 shows the *region of potential sensitivity*, within which at least 90% of the Monte Carlo experiments fail the null hypothesis. This clearly illustrates the sensitivity of the null test. The limits to our sensitivity to an axion signal, or any other unknown particle produced in this experiment and decaying to e^+e^- pairs are reflected by the boundaries of this plot. Sufficiently short-lived particles would decay too soon to show up directly in the length distribution. This accounts for the lower boundary of the figure. We are sensitive to both an exponentially decaying excess in the early length bins and to an overall excess of conversions in a particular mass bin. Studying the statistical significance of these excesses as a function of the number of pairs expected with a given mass generates the upper boundary shown. We lose sensitivity as the axion

mass decreases [as Eq. (1) shows the mixing decreases quadratically with axion mass] and as the lifetime increases so that fewer decays occur within 15 mm. We emphasize that this study is independent of the experimental data in the 1–15 mm region, and that it shows the anticipated sensitivity of our measurement prior to the execution of the experiment. We also show the effect of halving or doubling the assumed coupling to the π^0 .

Our *region of exclusion* was determined by comparing the theoretically expected distributions for different values of the axion lifetime and mass with the data. Two thousand Monte Carlo experiments were performed as above for each of a set of axion masses and lifetimes. The averages of these experiments at each mass and lifetime gave smoothed representations of the expected axion length distribution. When added as above to the expected distribution for photons from π^0 decays (see appendix for details), we obtained a prediction for a length distribution containing the specified axion. Note that a mass cut was applied. Figure 6, which compares the mass distribution of our data with what it would look like if an 8 MeV axion with lifetime 10^{-13} sec existed, shows the value of this cut. Comparing to the data, we rejected the hypothesis of an axion with the assumed parameters with 90% confidence when the χ^2 exceeded 21.1. As an example, Fig. 7 shows the comparison of the data with the theory once mass cuts have been applied for three different axion models [curves (a), (b) and (c)]. We reject models (b) and (c) and we are insensitive to model (a). The χ^2 of the data against this average distribution was computed for many different sets of axion parameters; the region over which the χ^2 exceeded 21.1 is shown in Fig. 8. Table I shows, for various selected values of axion mass and lifetime, the number of axion decays which would be expected in the signal region and the number of e^+e^- pairs found (as well as listing other quantities of interest). Figure 8 shows our region

of exclusion, *i.e.*, that region in which there is only a 10% or smaller probability that an axion with the properties assumed would reproduce the data.

Our data cannot exclude the possibility that the object observed at GSI is an axion. However, with minimal assumptions, we exclude a large region of the parameter space available to such axions. We are also aware of the existence of limits on the production of such axions (coupling to u quarks) coming from studies of the $\pi^+ \rightarrow e^+ \nu e^+ e^-$ branching ratio.¹⁷ Our experiment can be considered a complementary approach; within our region of sensitivity we confirm these more stringent limits. In addition, our limit applies to the existence of any particle coupling to a π^0 and decaying to e^+e^- pairs. Figure 9 shows the range of couplings of such a particle to the π^0 , which we exclude as a function of the ratio of the particle's mass to its lifetime.

IV. SUMMARY

If there is an axion variant which mixes with the π^0 , has a short lifetime (4.6×10^{-13} sec in the Krauss and Wilczek model), and decays into e^+e^- pairs, then the expected signal in our experiment for such an axion would be an excess of e^+e^- pairs at short lengths from the production vertex. Although we are not sensitive to the 1.8 MeV enhancement seen at GSI, our result does restrict greatly the allowed parameter space for such variant axions. As shown in Fig. 8, we see no sign of such an axion for masses above 4 MeV and lifetimes in the range $10^{-15} < \tau < 10^{-11}$ sec. The existence of any particle with a coupling to the π^0 and a decay to e^+e^- is also excluded for a range of particle mass/lifetimes and couplings as shown in Fig. 9.

V. ACKNOWLEDGMENTS

We thank Mike Peskin and Marek Karliner of the SLAC Theory Group for suggesting this use for our data.

We also thank the SLAC bubble chamber crew and the scanning teams at all the participating laboratories for their efforts. We are grateful to the groups at Duke University, Florida State University, KEK Japan, MIT, Nara Women's University Japan, Technion-Israel Institute of Technology, University of Tel Aviv and the Weizmann Institute for the data from BC72. Finally, we also thank Steve Tether and Dick Yamamoto of MIT and Avi Yagil of Technion for their assistance in collecting the data.

APPENDIX

We have developed a Monte Carlo experiment to study the BC75 data in two different ways. This study requires three inputs:

- (1) the predicted length distribution for axions;
- (2) the measured mass distributions for gammas and that predicted for axions;
- (3) the number of π^0 's producing axions for an assumed axion mass (m_a) and life-time (τ_a).

A. The length simulation

The length distribution for γ 's is assumed to be given by:

$$\frac{dN_\gamma}{dl} = [7/(9l_0)] N_\gamma^{tot} e^{-7l/9l_0} \quad , \quad (A1)$$

where $l_0 \approx 1100$ cm is the radiation length for gammas (an allowance was made for the conditions under which we operated the bubble chamber). Similarly, the length distribution for axions is assumed to be:

$$\frac{dN_a}{dl} = m_a/p_a \tau_a N_a^{tot} e^{-m_a l/p_a \tau_a} \quad . \quad (A2)$$

For each axion, a momentum p_a is chosen. The axions are assumed to have the same momentum distribution as π^0 's.¹⁸

B. The e^+e^- mass distribution simulation

(1) *The gamma mass measurement distribution*

The gamma mass measurement distribution in the Monte Carlo is based on a sample of e^+e^- pairs with mass less than 30 MeV from the BC72/73 DST (11,283 pairs

in total). We performed a fit to this mass distribution and found it fits well to the function

$$\frac{dN_\gamma}{dm} \propto \int e^{-\frac{(m^2 - m_{e^+e^-}^2)^2}{2\sigma_{m^2}^2}} \times f(\sigma_{m^2}, \sigma_{m^2}^*) d\sigma_{m^2} \quad ;$$

with the weight function being given by

$$f(\sigma_{m^2}, \sigma_{m^2}^*) = \frac{b(p-1)}{(1+bX)^p} \quad ,$$

where $X = \sigma_{m^2} - \sigma_{m^2}^*$, and f is a normalized function, *i.e.*,

$$\int_{\sigma_{m^2}^*}^{\infty} f(\sigma_{m^2}, \sigma_{m^2}^*) d\sigma_{m^2} = 1 \quad ,$$

$m_{e^+e^-} = 1.022 \text{ MeV}/c^2$, and $\sigma_{m^2}^*$, p , b are fitting parameters. The fit to the distribution using the parameters

$$\sigma_{m^2}^* = 3.33 \text{ (MeV}/c^2)^2 \quad ; \quad p = 1.89 \quad ; \quad b = 0.0705 \text{ (MeV}/c^2)^{-2} \quad ,$$

is shown superimposed on the data in Figs. 2 and 3.

(2) The axion mass distribution

Having fit the data to obtain a function describing the gamma mass distribution, we assume that the same function will apply to the axion distribution if we replace $m_{e^+e^-}$ by the mass of the axion, m_a . We then have

$$\frac{dN_a}{dm} \propto \int e^{-\frac{(m^2 - m_a^2)^2}{2\sigma_{m^2}^2}} \times f(\sigma_{m^2}, \sigma_{m^2}^*) d\sigma_{m^2} \quad .$$

We assume that the constants obtained in the fit to the BC72/73 gamma data continue to apply.

C. The mixture of π^0 's and axions

We use the number of e^+e^- pairs observed in the 40–200 mm region (N_{obs}^{long}) in BC72/73 to arrive at an expected number of γ conversions and axion decays in BC75. We do not correct for Dalitz decays or for the production of γ from η decays (we did, however, estimate that these made less than a 2% reduction to the number of axion decays expected). Our analysis does correct for the presence of photons from axion decays in the control region. The number of γ conversions is given by:

$$N_{\gamma}^{tot} = f \frac{1.988 N_{obs}^{long}}{1.988 Pr(\gamma^{long}) + \xi_{\pi^0}^2 (Pr(a^{long})) / (1 - \xi_{\pi^0}^2)} ,$$

and the number of axion decays is

$$N_a^{tot} = \frac{N_{\gamma}^{tot} \xi_{\pi^0}^2}{1.988 (1 - \xi_{\pi^0}^2)} ,$$

where $\xi_{\pi^0}^2 \approx 1/2(m_a/m_{\pi^0})^2$ is the coupling constant, $Pr(\gamma^{long}) = [-e^{-7l/9l_0}]_{40 \text{ mm}}^{200 \text{ mm}}$, $Pr(a^{long})$ is the probability of an axion decaying in the 40–200 mm region, and f is the relative normalization between the BC72/73 and BC75 data (approximately 1). Figure 6 shows an example of the distribution obtained, assuming the existence of an 8 MeV axion.

D. Monte Carlo method to produce sensitive and excluded regions

We assume the existence of an axion with a certain (m_a, τ_a) . We select a range of measured masses about m_a that would include about 60 to 70% of the axions. The exact range is a compromise of signal to noise. We exclude all short pairs (from $N_{\gamma}^{short} = 277$ for BC75) with mass outside this region, and build a length histogram called the *data length distribution* in fourteen “1 mm” bins (for the short region, *i.e.*,

1–15 mm). We also build a theoretical length histogram (same type) with mass cuts, for the hypothesis of no axion existence (called H^0 or *Null Hypothesis*). This is a smooth theoretical prediction with no fluctuations.

For each assumed (m_a, τ_a) , we generate 2000 Monte Carlo experiments, by selecting a number of γ 's (N_γ) and a number of axions (N_a) according to expectations. Then we convert the γ 's in the short region according to Eq. (A1), and allow the axions to decay anywhere according to Eq. (A2).

For each Monte Carlo experiment, we build a length histogram (same type as the one for H^0) for the decays and conversions in the short region (*i.e.*, both γ 's and axions), and then we compare this histogram to H^0 . This tells us whether or not the results of that particular Monte Carlo experiment fail the H^0 . A failure requires the χ^2 to exceed 21.1 (the 90% confidence level for 14 degrees of freedom). The sensitive region is where 90% or more of the 2000 experiments fail. We interpret this to mean our experiment can detect deviations from H^0 in this region.

To get the excluded region (the second method), for each assumed (m_a, τ_a) point, we average the length distributions over the 2000 Monte Carlo experiments. This gives us a theoretical *axion-gamma model* distribution for that particular point. We can now compare the model to the observed data length distribution. This enables us to determine how well this particular axion model reproduces the data. We exclude with 90% confidence a region of (m_a, τ_a) space where $\chi^2 \geq 21.1$. This region of exclusion, our final result, gives the range of axion masses and lifetimes rejected by our experimental measurements. Table I gives some of the numerical results obtained using this method.

REFERENCES

1. R. D. Peccei and H. R. Quinn, *Phys. Rev. Lett.* **38**, 1440 (1977).
2. Experimental limits on CP violation in strong interactions, such as those from measurements of the neutron electric dipole moment, place limits on this phase angle of $\theta < 10^{-9}$.
3. A. Zehnder, *Proc. 1982 Gif-sur-Yvette Summer School*;
S. Yamada, *Proc. 1983 Lepton-Photon Symposium*, Cornell (1983);
Y. Asano *et al.*, *Phys. Lett.* **107B**, 159 (1981).
4. M. Dine, W. Fischler, and M. Srednicki, *Phys. Lett.* **104B**, 199 (1981).
5. T. Cowan *et al.*, *Phys. Rev. Lett.* **54**, 1761 (1985); **56**, 444 (1986).
6. R. D. Peccei, T. T. Wu, and T. Yanagida, *Phys. Lett.* **172B**, 435 (1986).
7. L. M. Krauss and F. Wilczek, *Phys. Lett.* **173B**, 189 (1986).
8. T. Bowcock *et al.*, *Phys. Rev. Lett.* **56**, 2676 (1986);
G. Margeras *et al.*, *Phys. Rev. Lett.* **56**, 2672 (1986).
9. M. Suzuki, *Phys. Lett.* **175B**, 364 (1986).
10. S. Weinberg, *Phys. Rev. Lett.* **40**, 223 (1978).
11. Estimates give about $4 \text{ MeV}/c^2$ for m_u and $7 \text{ MeV}/c^2$ for m_d ; for example, see
J. Gasser and H. Leutwyler, *Phys. Rev.* **87C**, 77 (1982).
12. Some models do, in fact, make this coupling vanish. One such model is discussed
by L. M. Krauss and D. J. Nash [*Phys. Lett.* **B202**, 560 (1988)], but in this
case the axion is too light to decay to e^+e^- and we would not in any case be
sensitive to it.

13. M. Karliner and M. Peskin, private communication.
14. K. Abe *et al.*, *Phys. Rev.* **D33**, 1 (1986) and references therein.
15. K. Abe *et al.*, *Phys. Rev. Lett.* **48**, 1526 (1982).
16. Some improvements, mainly related to optical resolution, were made to the apparatus used for BC75 (details can be found in Ref. 14), but these do not affect the validity of our use of the BC72 data. Small differences in triggering efficiency, for example, were corrected for.
17. These limits are due to a theoretical analysis by Krauss and Wise [L. M. Krauss and M. B. Wise, *Phys. Lett.* **176B**, 483 (1986)], and are based on an experimental result due to the SINDRUM collaboration [R. Eichler *et al.*, *Phys. Lett.* **175B**, 10 (1986)].
18. This was taken to be the same as the π^- momentum distribution given in the unpublished thesis of V. R. O'Dell, Brown University (May 1987), which was based on data from BC72. Although the mass of the axion is different from that of a pion, both masses may be considered small when compared to the momentum transfers involved in their production, and so both should have similar momentum distributions.

FIGURE CAPTIONS

1. Scanning efficiency as a function of conversion or decay length.
2. Mass distribution for all photon pair conversions between 40–200 mm of the primary vertex (BC72/73 data, points with error bars). The solid line curve is a fit to the data used in our Monte Carlo analysis.
3. Mass distribution for photon pair conversions between 1–15 mm from the primary event vertex (BC75). The solid line curve is a fit to the data used in our Monte Carlo analysis.
4. Length distribution for photon pair conversions between 1–15 mm from the primary event vertex.
5. Region of sensitivity for various assumed axion coupling strengths [standard (a), double (b), and half (c)]. This plot shows the region of mass and lifetime space in which we can search for axions (for more details, see text).
6. Monte Carlo mass distribution of e^+e^- pairs assuming production of a specific axion as well as gamma conversions (solid line) compared to the data (points with error bars).
7. Three theoretical axion length distributions are compared to the data. The mass (and hence the coupling) is kept fixed and the lifetime is varied; (a) is not excluded by the data, but (b) and (c) are.
8. Regions of exclusion as a function of the axion coupling. These are the regions of mass–lifetime space for which our data excludes axion production (for more details, see text).

9. Region of exclusion as a function of the axion's mass/lifetime compared to its coupling to π^0 's.

Table I. Numerical results for selected axion masses and lifetimes giving number of expected pairs due to axion decay in region of interest.

AXION MASS (MeV/c**2)	AXION LIFETIME (s)	Number of gammas expected (1-15 mm region)	Number of axions which would decay in 1-15 mm region	Null hypothesis χ^2 probability	χ^2 compared to data
28.000	0.5E-15	0.30	0.00	0.0000	0.0000
28.000	0.2E-14	0.30	4.43	0.9890	4.4320
28.000	0.1E-13	0.30	144.99	1.0000	144.9894
28.000	0.4E-12	0.28	939.55	1.0000	939.5479
28.000	0.5E-11	0.22	283.36	1.0000	283.3586
20.000	0.5E-15	0.78	0.00	0.1660	0.6860
20.000	0.2E-14	0.78	6.71	0.9970	7.4025
20.000	0.1E-13	0.78	110.95	1.0000	111.6563
20.000	0.2E-12	0.76	517.60	1.0000	518.2969
20.000	0.9E-12	0.70	346.65	1.0000	347.3118
14.000	0.5E-15	3.06	0.12	0.1690	9.2499
14.000	0.4E-14	3.06	26.59	1.0000	32.0345
14.000	0.1E-12	3.04	258.39	1.0000	257.1799
14.000	0.6E-11	2.84	51.24	1.0000	50.3596
14.000	0.1E-10	2.87	36.32	1.0000	35.6213
10.000	0.5E-15	9.99	0.19	0.1340	7.5762
10.000	0.4E-14	9.99	22.34	1.0000	28.1765
10.000	0.1E-12	9.93	137.16	1.0000	139.2160
10.000	0.2E-11	9.57	45.59	1.0000	48.0622
10.000	0.8E-11	9.66	18.20	0.9875	21.8426
8.000	0.5E-15	21.12	0.28	0.1055	9.0801
8.000	0.2E-14	21.12	7.50	0.7955	15.4031
8.000	0.1E-12	21.02	89.70	1.0000	89.2559
8.000	0.2E-11	20.54	26.26	0.9835	28.3326
8.000	0.8E-11	20.71	10.55	0.5935	15.3567
6.000	0.5E-15	53.43	0.42	0.0975	10.7410
6.000	0.8E-14	53.43	28.08	0.9920	30.2255
6.000	0.3E-13	53.40	50.32	1.0000	43.7711
6.000	0.1E-12	53.21	51.17	1.0000	41.4428
6.000	0.2E-11	52.63	13.40	0.4245	15.0445
5.000	0.5E-15	93.57	0.49	0.1085	17.3328
5.000	0.3E-14	93.57	10.08	0.4705	23.6300
5.000	0.3E-13	93.52	37.25	0.9695	30.6187
5.000	0.2E-12	92.97	29.45	0.7540	21.3339
5.000	0.7E-11	92.95	3.57	0.1185	16.4724
4.000	0.5E-15	169.00	0.55	0.1175	12.5534
4.000	0.3E-14	169.00	8.49	0.2680	15.5551
4.000	0.3E-13	168.90	25.97	0.5715	18.7375
4.000	0.2E-12	168.21	18.48	0.2925	13.4752
4.000	0.7E-11	168.36	1.97	0.1195	12.4271
3.000	0.5E-15	208.56	0.63	0.1190	9.5273
3.000	0.3E-14	208.56	6.23	0.2000	10.1739
3.000	0.3E-13	208.45	14.99	0.2705	9.8869
3.000	0.2E-12	207.92	9.36	0.1715	8.6168
3.000	0.7E-11	208.17	0.91	0.1135	9.1122

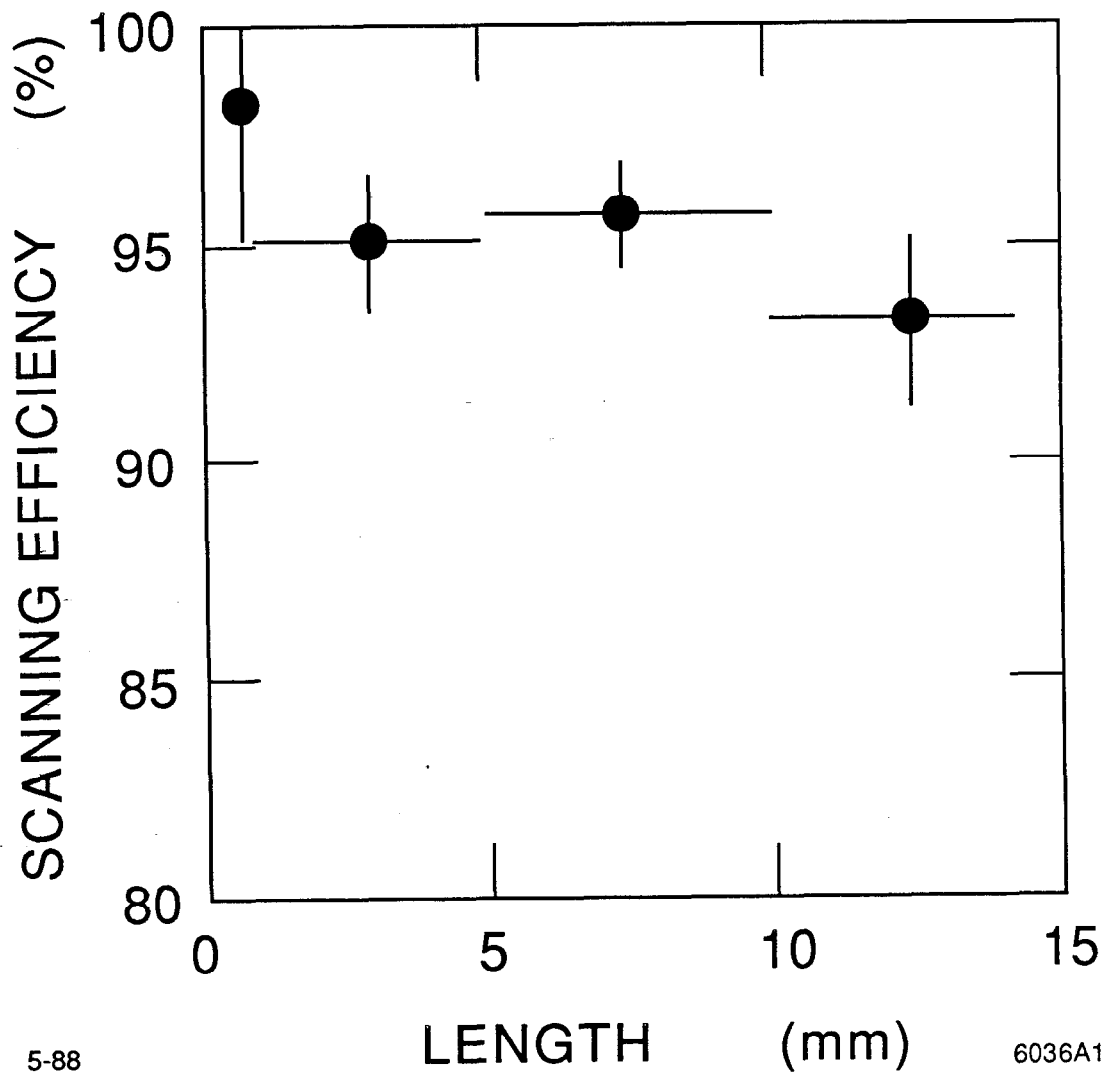
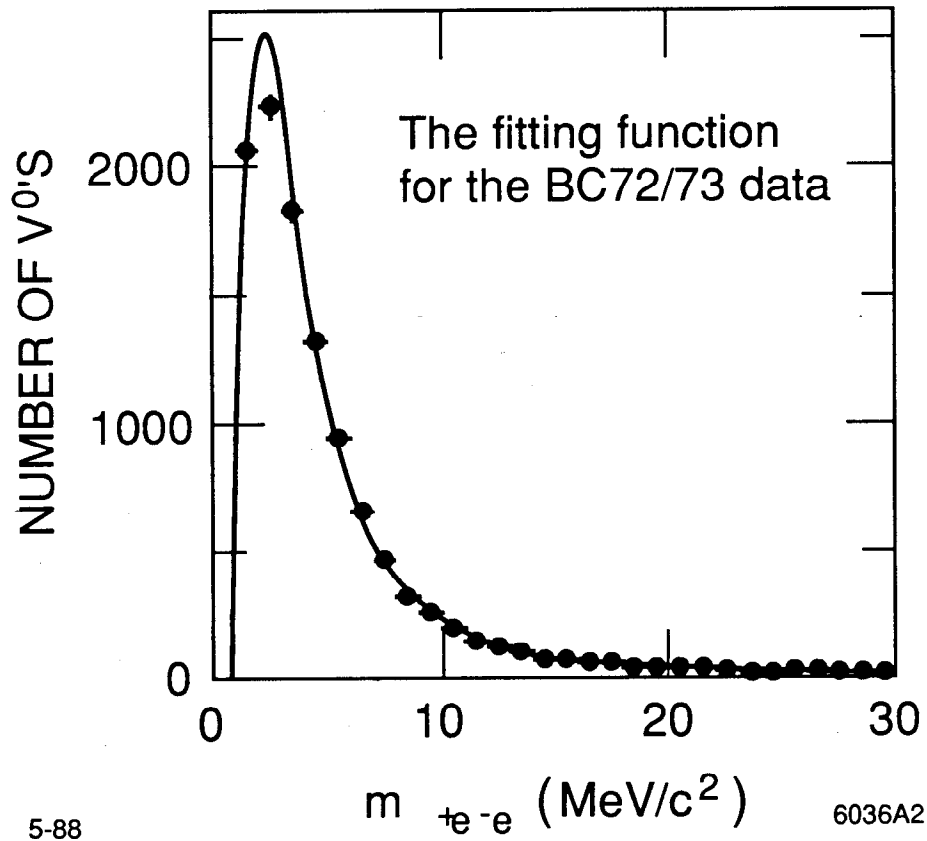


Fig. 1



5-88

6036A2

Fig. 2

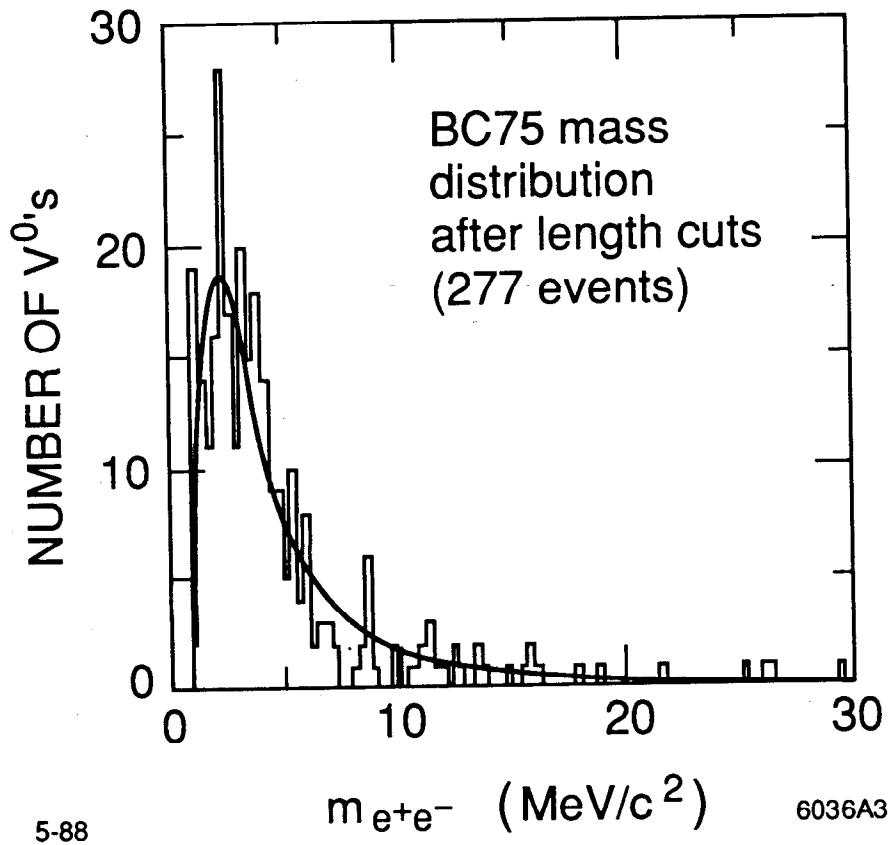


Fig. 3

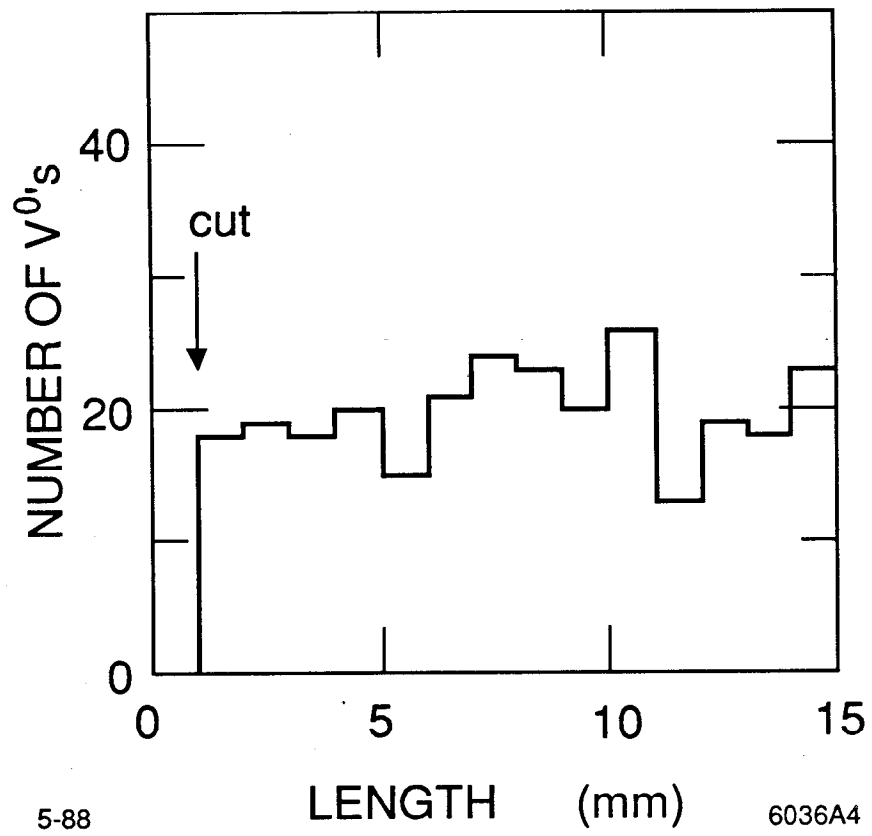


Fig. 4

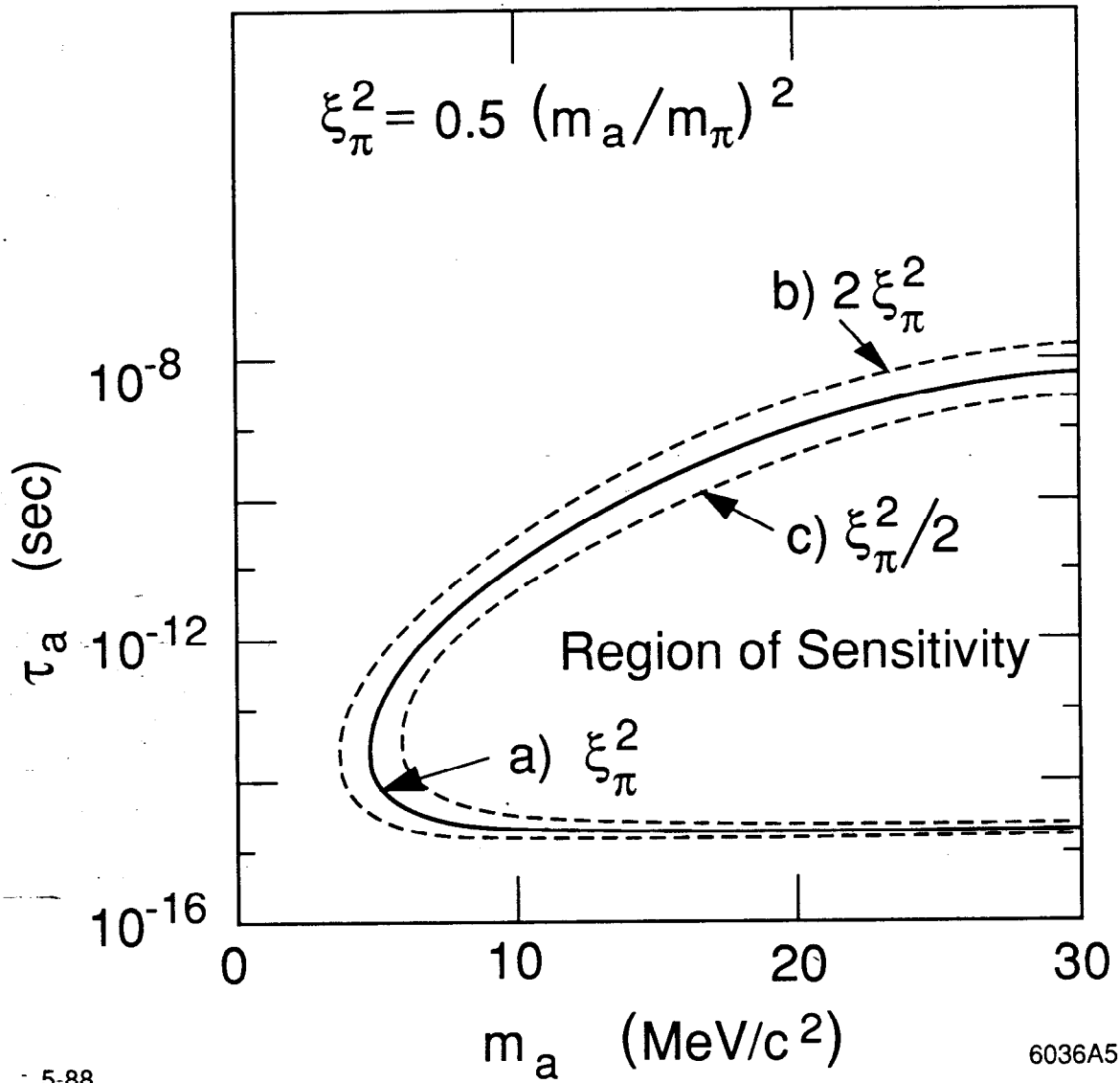


Fig. 5

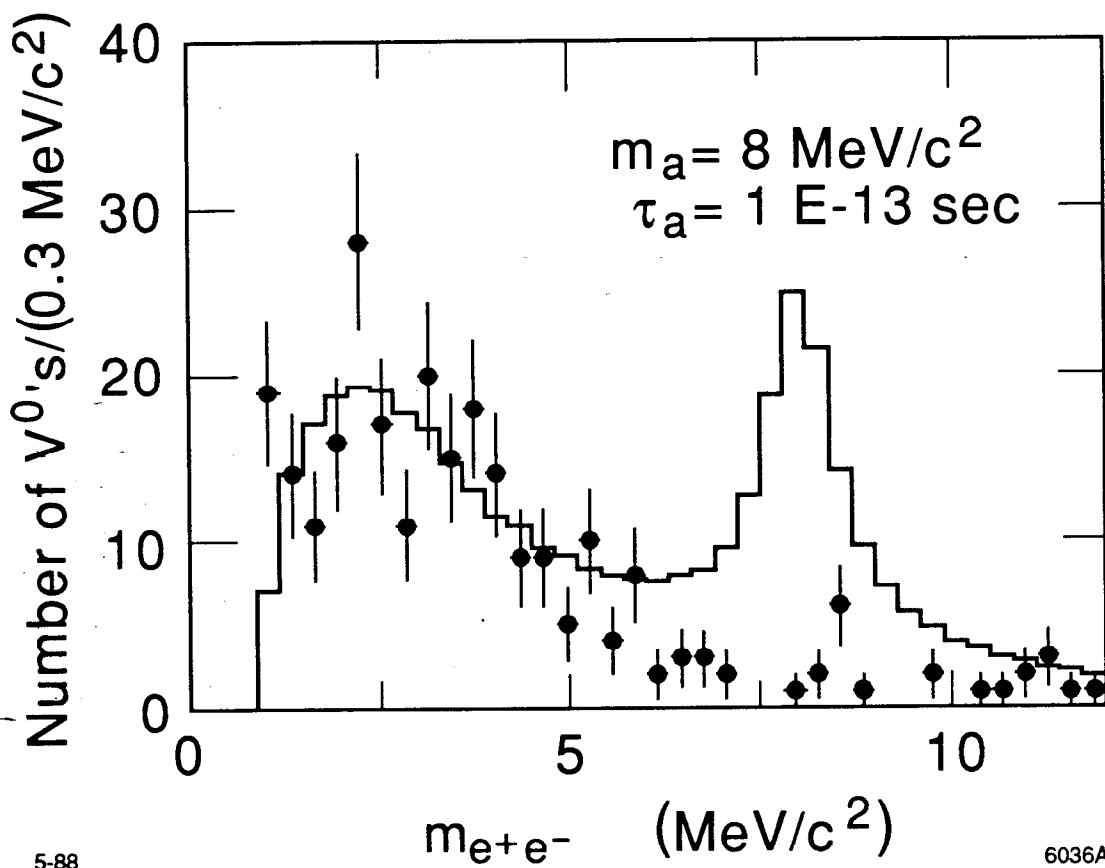


Fig. 6

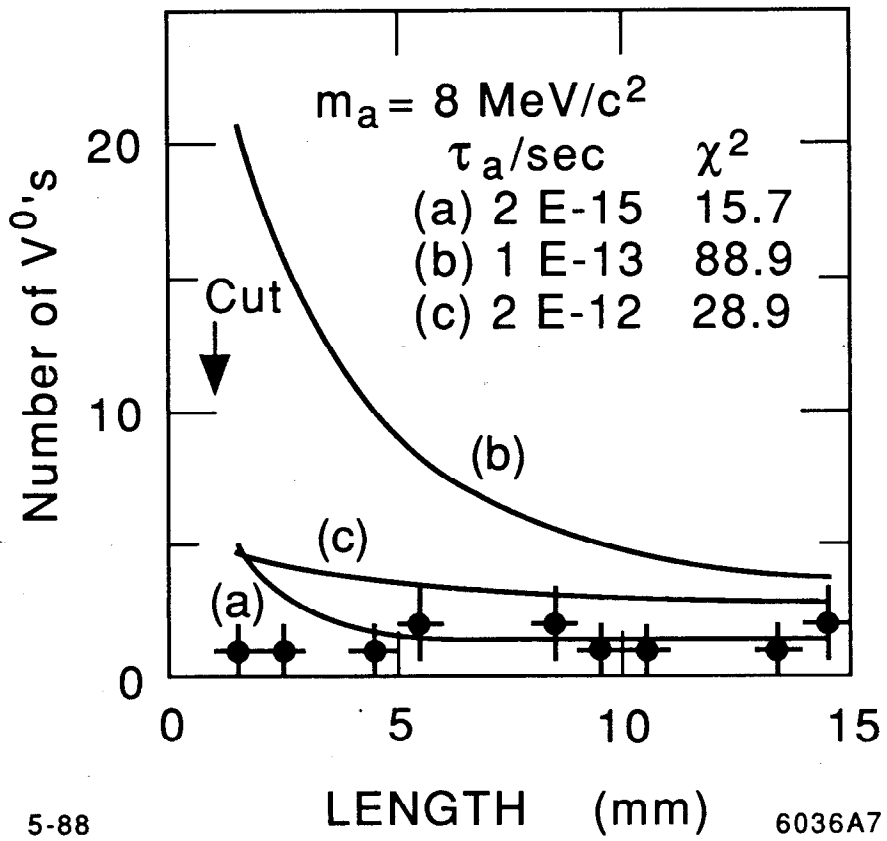


Fig. 7

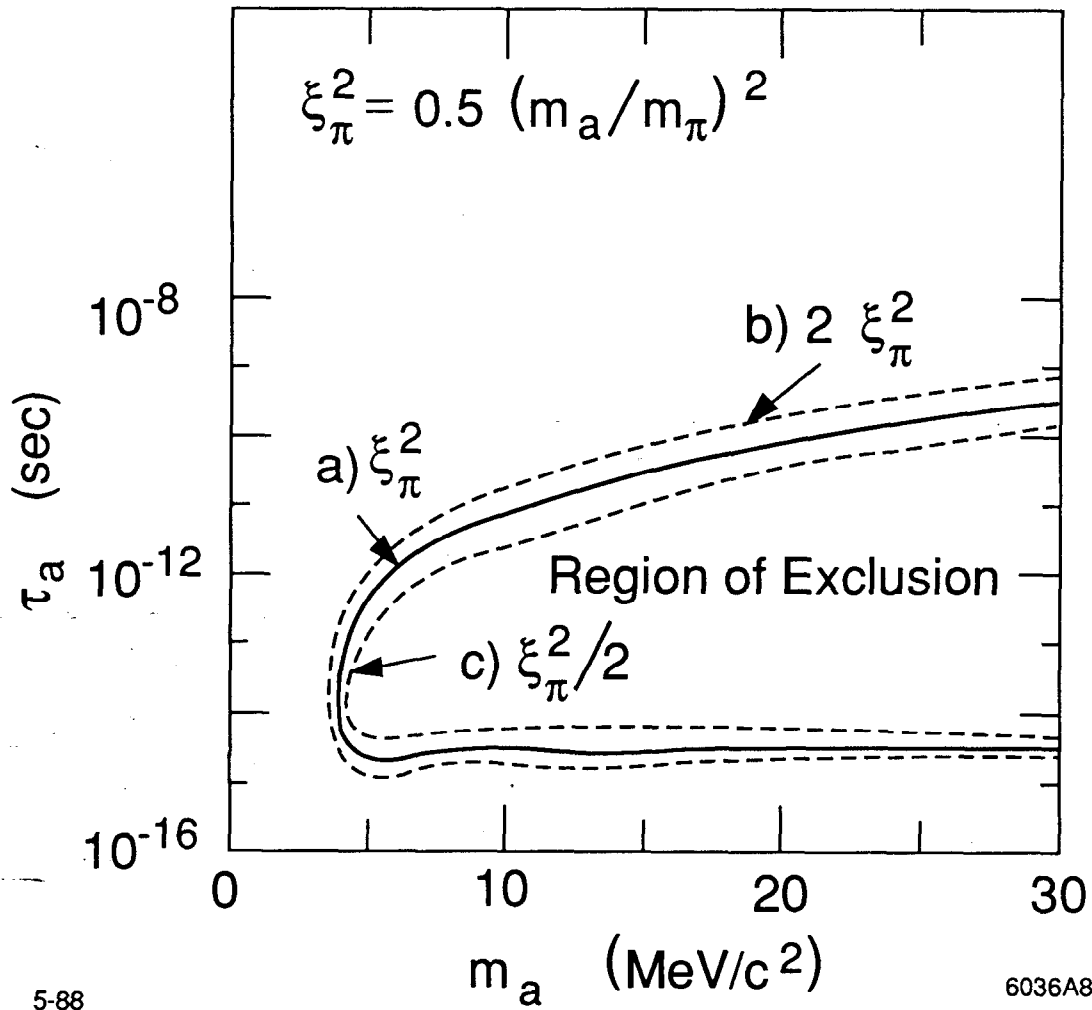
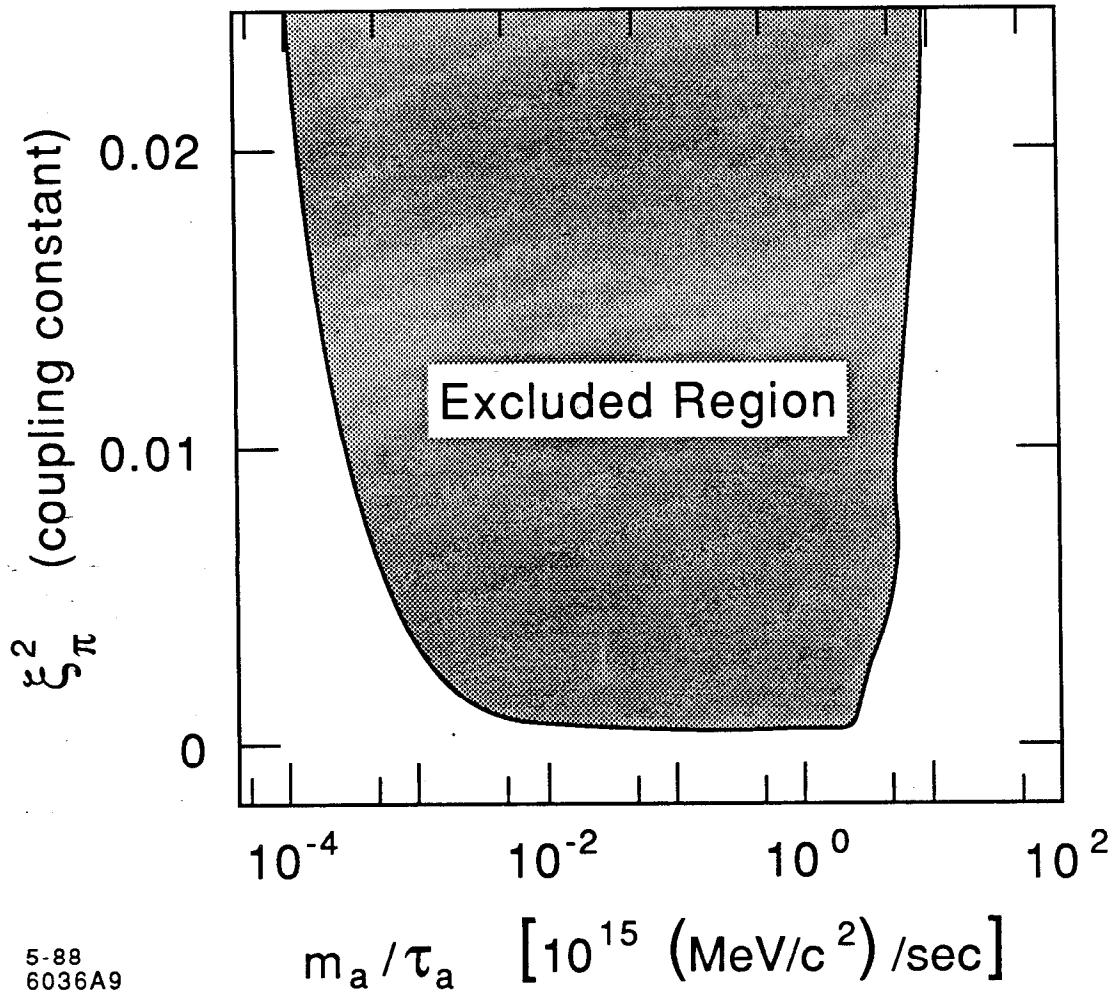


Fig. 8



5-88
6036A9

Fig. 9